View metadata, citation and similar papers at core.ac.uk

brought to you by CORE

provided by IntechOpen

We are IntechOpen, the world's leading publisher of Open Access books Built by scientists, for scientists

4,800
Open access books available

122,000
International authors and editors

135M
Downloads

Our authors are among the

154
Countries delivered to

TOP 1%
most cited scientists

12.2%
Contributors from top 500 universities

CLARIVATE ANALYTICS BOOK CITATION INDEX INDEXED

WEB OF SCIENCE™

Selection of our books indexed in the Book Citation Index in Web of Science™ Core Collection (BKCI)

Interested in publishing with us?
Contact book.department@intechopen.com

Numbers displayed above are based on latest data collected.
For more information visit www.intechopen.com

Chapter 6

A Comparison of Mass Transfer Coefficients between Rotating Magnetic Field Mixer and Stirred Tank Reactor

Grzegorz Story, Marian Kordas and Rafał Rakoczy

Additional information is available at the end of the chapter

http://dx.doi.org/10.5772/61059

Abstract

The mass transfer process is the subject of many experimental studies in chemical engineering and also one of the most commonly used processes. Unfortunately, the mechanism of this process is still not fully understood, especially when nonstandard methods of intensification of mass transfer are used. In this investigation, the use of an alternating magnetic field action (AMFs) causing mass transfer was taking into consideration. As a result of the flow of electrically conductive fluid near the alternating magnetic field, electromagnetic forces can be generated within the liquid. These forces arise as a result of interaction between the magnetic field and the electric current. They are responsible for the rotation and consequently cause movement of the fluid on which they act. Therefore, there is the possibility of using these properties in the construction of a nonintrusive mixing stirrer.

The aim of this study is to determine the mixing time, the power consumption and the mixing efficiency in the mass transfer process that is induced under the action of RMF. The present study compared the mass transfer coefficient of two reactor types: RMF mixer and stirred tank reactor.

Keywords: Rotating magnetic field, mixing energy, mass transfer

1. Introduction

The mass transfer process is the subject of many experimental studies in chemical engineering and also one of the most commonly used processes. Unfortunately, the mechanism of this

INTECH
open science | open minds

© 2015 The Author(s). Licensee InTech. This chapter is distributed under the terms of the Creative Commons Attribution License (http://creativecommons.org/licenses/by/3.0), which permits unrestricted use, distribution, and reproduction in any medium, provided the original work is properly cited.

process is still not fully understood, especially when nonstandard methods of intensification of mass transfer are used. In this investigation, the use of an alternating magnetic field action (AMFs) causing mass transfer was taken into consideration. In many industries, static magnetic fields (MSSF) are mainly used as magnetic separators or electromagnetic brakes, while transverse rotating magnetic fields (TRMFs) are used in asynchronous electric motors or as an electromagnetic stirrer. As a result of the flow of electrically conductive fluid near the alternating magnetic field, electromagnetic forces can be generated within the liquid. These forces arise as a result of interaction between the magnetic field and the electric current, and they are called Lorentz or Laplace forces. They are responsible for the rotation and consequently cause movement of the fluid on which they act. Therefore, there is the possibility of using these properties in the construction of a nonintrusive mixing stirrer. The use of rotating magnetic field (RMF) acting on the conductive fluid is mainly used in the crystallization process and other processes in chemical engineering.

The application of the TRMF in chemical engineering processes has many advantages. Instead of using a mechanical mixer to increase the process intensity, it is possible the use static or rotating magnetic field (RMF). Generally, it is known that small particles having magnetic properties are arranged along the magnetic field lines and that they are also moving with movement of the magnetic field. The use of TRMF creates the possibility of using these particles and also controlling the hydrodynamic state of the magnetodispersion. Magnetic particles in the system, which are subjected to the influence of magnetic field, will behave as active microstirrers. Usually, the mixing process is carried out in the mixing tank or stirred vessel. The process performance can be evaluated on the basis of energy consumption and mixing time. However, when choosing the proper mixing equipment, the mixing time and energy of the system should not be considered separately. The minimum value of the mixing energy determines the optimum process conditions. Therefore, it is desirable to know value of the mixing energy during the design of the mixing device.

The aim of this study are to determine the mixing time, the power consumption and the mixing efficiency in the mass transfer process (dissolution of NaCl-cylindrical sample) that is induced under the action of RMF. The present study compared the mass transfer coefficient of two reactor types: RMF mixer and stirred tank reactor (STR) equipped with Rushton turbine. It is decided that in the present report, the influence of the mixing system consisting of the RMF generator or the mechanical stirrer on the mass transfer process is described by applying the nondimensional parameters, like Sherwood, Schmidt, and Reynolds numbers, and mixing energy. Mixing energy was calculated as a product of the mixing time and power input to the mixing liquid. These dimensionless numbers allow quantitative representation and characterization of the influence of the hydrodynamics state under the various hydrodynamic conditions on the mass transfer rate. The dimensionless groups are used to establish the effect of the various types of the mixing process on this operation in the form of the dimensionless correlation. Moreover, the comparison of the amount of energy input to reach the same mass transfer rate with two different devices (RMF mixer and STR) is discussed.

http://dx.doi.org/10.5772/61059

2. Theoretical background

There is one way of looking at the intensity of the external mass transfer, namely, the criterion of Sherwood, *Sh*. The physical meaning of the dimensionless Sherwood number lies in relating the actual flow of the component from boundary layer to the transverse flow in the stationary liquid layer with characteristic *L* dimension in accordance with concentration difference of this component. A relationship for the mass transfer process under convective conditions, based on the analogy to the heat transfer process, may be expected as a relationship between three dimensionless numbers, as follows [1]:

$$Sh = f\left(Re, Sc\right) \tag{1}$$

where

$Sh = \frac{(\beta)_V d_s^2}{\rho D}$ —dimensionless Sherwood number;

$Sc = \frac{v}{D}$ —dimensionless Schmidt number;

$Re = \frac{w\, l\, \rho}{\eta}$ —dimensionless Reynolds number.

In Eq. (1), a major role in mass transport has the following dimensionless numbers: Sherwood and Schmidt numbers. The first one (Sherwood number) describes the ratio of convective to diffusive mass transport [2], while the second one (Schmidt number) indicates physical parameters important for the analyzed setup. Furthermore, the Schmidt number is also the measure of the mass and momentum transport relative effectiveness by diffusion. In the basic Eq. (1), except the Sherwood and Schmidt numbers, additionally the Reynolds number can be found. The Reynolds number represents the ratio of convective to viscous momentum transport. The value of the Reynolds number determines the existence of laminar or turbulent regime of fluid flow. For small values of the Reynolds number, viscous forces are sufficiently large relative to inertia forces, and we have laminar flow. With increasing values of the Reynolds number, viscous effects become progressively less important relative to inertia effects, and we have turbulent flow.

It is clear that Eq. (1) in present form cannot be practical use. First, it must be rendered quantitative. It can be achieved by assuming that the functional relation is in the following form [3,4]:

$$Sh = aRe^b\, Sc^c \tag{2}$$

This is commonly known that the coefficient of the mass transfer process can be calculated using three dimensionless groups: Sherwood, Reynolds, and Schmidt numbers. Using Eq. (2),

it is possible to combine a lot of data obtained from experimental measurements for many different operations. The *a*, *b*, and *c* coefficients of Eq. (2) are determined experimentally on the basis of the results of the measurements. Under forced convection conditions, this relationship can be presented in the form of [5]

$$Sh \propto Re^{0.5} Sc^{0.33} \tag{3}$$

The exponent upon of the Schmidt number is to be 0.33 [6–10] as there is some theoretical and experimental evidence for this value [11], although reported values vary from 0.56 [12] to 1.13 [13].

It should be also noted that for the mass transfer process under natural convection conditions, i.e., then, when the Reynolds number is unimportant, the general expression for the mass transfer has the following form:

$$Sh = f\left(Gr, Sc\right) \tag{4}$$

However, in the presented report, the mass transfer process proceeds under convective conditions; therefore, it is described by means of the following relationships:

- For the stirred vessel equipped with the mechanical stirrer $\left(\text{the Rushton turbine}\right)$,

$$Sh = f\left(Re_{STR}, Sc\right) \quad \Rightarrow \quad \left[\frac{\left(\beta\right)_V \left(\left\langle d_s \right\rangle\right)^2}{\rho D}\right] = f\left\{\left[\frac{n d_m^2}{\nu}\right], \left[\frac{\nu}{D}\right]\right\} \qquad \text{a}$$

- For the stirred vessel equipped with the RMF generator, $\left(5\text{b}\right)$

$$Sh = f\left(Re_{RMF}, Sc\right) \quad \Rightarrow \quad \left[\frac{\left(\beta\right)_V \left(\left\langle d_s \right\rangle\right)^2}{\rho D}\right] = f\left\{\left[\frac{w_{\text{RMF}} D_{\text{con}}}{\nu}\right], \left[\frac{\nu}{D}\right]\right\} \quad \text{b} \tag{5}$$

The above dimensionless groups were calculated with the psychical properties of the tested fluid in the temperature 20°C. In this paper, we present results of the mass transfer process using similar dimensionless groups. In this case, the relationship between Sherwood number and two other numbers, which inform about hydrodynamic conditions in the system, Reynolds and Schmidt numbers, was slightly modified. The Reynolds numbers for the process realized with using the STR or RMF were defined by the following equations, respectively:

$$Re_{STR} = \frac{n d_m^2}{\nu_l} \tag{6}$$

$$Re_{RMF} = \frac{w_{\phi_{\max}} D_{con}}{\nu_l} \tag{7}$$

http://dx.doi.org/10.5772/61059

where

$$w_{\phi_{\max}} = B_{\max} D_{con} \sqrt{\frac{\omega_{RMF} \sigma_e}{\rho_l}}, \ \mathrm{m \cdot s^{-1}} \tag{8}$$

In order to establish the effect of the hydrodynamic conditions on the mass transfer process in the tested experimental setups, we propose the following relationship:

$$\frac{Sh}{Sc^c} = aRe^b \tag{9}$$

The effect of mass transfer process can be described by using the variable $ShSc^{-c}$ proportional to the term aRe^b.

One of the parameters that describe the mixing process is the mixing time. This parameter determines the time needed to obtain required level of the mixture homogeneity. Therefore, the mixing time is a contractual value and depends on the mixture homogeneity definition. The homogenization time is often describe with a nondimensional module, defined as a required rotational impeller speed to obtain expected value of the mixing system homogeneity. Mixing time can be expressed as follows:

$$\Theta = \frac{\tau_{mix} \upsilon_0}{l_0^2} \tag{10}$$

To measure the level of the mixture homogeneity, the techniques based on put the system out of equilibrium are frequently used. Afterward, the time in which system returns to the equilibrium state is measured. Usually, one of the two techniques is used: a method that relies on the conductivity measurements [14–17] or thermal method [18,19]. Both of them are characterized by easy conduct of the experiment, and there are also relatively cheap. The conductometric method is based on adding to the system impulse influencing the change in the electrical conductivity of the mixed liquor. The second method is based on adding to the system signal in the form of the hot liquid. In this work, the thermal method of put the system out of equilibrium was used.

Another important parameter that determines the system cost of the process is the power consumption. This parameter can be used as a measure of energy consumption in the process. Power consumption for the mixing process can be calculated on the basis of the relationship between dimensionless number [20,21] as follows:

$$Ne = f\left(Re\right) \tag{11}$$

where Newton number is defined as

$$Ne = \frac{P_0}{n_0^2 l_0^5 \rho_0} \tag{12}$$

In the case of using a mechanical stirrer, n is defined as a frequency of rotation of the agitator, and a linear dimension, l_0, is substituted as a diameter of the stirrer, d_m.

In the case of influence, the rotating magnetic field n is defined as an angular velocity of the liquid, which is under the action of the RMF in the container, $n = \Omega_l D_{con}$. The magnetic Newton number, Ne_m, is describe as

$$Ne_m = \frac{P_0}{\left(\Omega_l D_{con}\right)^3 D_{con}{}^5 \rho_l} \tag{13}$$

Where

$$\Omega_{RMF} = \frac{w_{\phi_{\max}}}{D_{con}},\ \mathrm{s}^{-1} \tag{14}$$

The Reynolds numbers for the process realized with using the STR or RMF were defined before (Eqs. 6–8).

A parameter that connects both mixing time and power consumption is a mixing energy [22–26]. This parameter is defined as the product of the mixing time in relation to the volume of mixed liquor and power input:

$$e_{mix} = \tau_{mix} P_a,\ \mathrm{J} \tag{15}$$

This parameter can be presented as a dimensionless number:

$$e^*_{mix} = a_3 Re^{3+b_3} C^{b_3} \tag{16}$$

By calculating the dimensionless value of the mixing energy, it is possible to compare the efficiency of mixing between different systems.

To calculate dimensionless mixing energy for the both systems (Eq. 16), some relationships must be designated. First, from the measured experimental data of the mixing time, a function must be plotted. Then the approximation curve must be designated in the form of the following equations:

http://dx.doi.org/10.5772/61059

$$\Theta_{RMF} = a_1 Re_{RMF}^{\ b_1} \quad \text{a}$$
$$\Theta_{STR} = a_1 Re_{STR}^{\ b_1} \quad \text{b} \tag{17}$$

Second, from the measured experimental data of the power consumption, a function given by the Eq. (11) must be plotted. Then the approximation curve must be designated in the form of the following equations:

$$Ne_{RMF} = a_2 Re_{RMF}^{\ b_2} \quad \text{a}$$
$$Ne_{STR} = a_2 Re_{STR}^{\ b_2} \quad \text{b} \tag{18}$$

Considering the resulting equations (Eq. 17) and rearranging terms to Eq. (10), the following equations were obtained:

$$\tau_{mix} = a_1 Re_{RMF}^{\ b_1} \left(\frac{D_{con}^{\ 2}}{\nu_l} \right), \text{ s} \quad \text{a}$$
$$\tau_{mix} = a_1 Re_{STR}^{\ b_1} \left(\frac{D_{con}^{\ 2}}{\nu_l} \right), \text{ s} \quad \text{b} \tag{19}$$

Substituting Eq. (12) into Eq. (18), we have

$$P_a = a_2 Re_{RMF}^{\ b_2} \left(\left(\Omega_{RMF} D_{con} \right)^3 D_{con}^{\ 2} \rho_l \right), \text{W} \quad \text{a}$$
$$P_{a,STR} = a_2 Re_{STR}^{\ b_2} \left(\left(n d_m \right)^3 d_m^{\ 2} \rho_l \right), \text{ W} \quad \text{b} \tag{20}$$

The obtained Eqs. (19) and (20) are then substituted in Eq. (15), and consequently we have the following relationships:

$$e_{mix} = \left[a_1 Re_{RMF}^{\ b_1} \left(\frac{D_{con}^{\ 2}}{\nu_l} \right) \right] \left[a_2 Re_{RMF}^{\ b_2} \left(\left(\Omega_{RMF} D_{con} \right)^3 D_{con}^{\ 2} \rho_l \right) \right], \text{ J} \quad \text{a}$$
$$e_{mix} = \left[a_1 Re_{STR}^{\ b_1} \left(\frac{D_{con}^{\ 2}}{\nu_l} \right) \right] \left[a_2 Re_{STR}^{\ b_2} \left(\left(n d_m \right)^3 d_m^{\ 2} \rho_l \right) \right], \text{ J} \quad \text{b} \tag{21}$$

Transforming Eq. (21), it may be given in the dimensionless forms, as follows:

$$
\begin{aligned}
& e_{mix} = \tau_{mix} P_a \Rightarrow \left[a_1 Re_{RMF}{}^{b_1} \left(\frac{D_{con}{}^2}{\nu_l} \right) \right] \left[a_2 Re_{RMF}{}^{b_2} \left(\left(\Omega_{RMF} D_{con} \right)^3 D_{con}{}^2 \rho_l \right) \right] \\
& \Rightarrow \left\{ \left(\frac{D_{con}{}^2}{\nu_l} \right) \left(\left(\Omega_{RMF} D_{con} \right)^3 D_{con}{}^2 \rho_l \right) \left(\frac{\nu_l^2}{\nu_l^2} \right) \right\} a_3 Re_{RMF}{}^{b_3} \qquad \text{a} \\
& \Rightarrow e_{mix} = a_3 Re_{RMF}{}^{3+b_3} \left\{ D \rho_l \nu_l{}^2 \right\} \\
& e^*_{mix} = a_3 Re_{RMF}{}^{3+b_3} C^{b_3} = \frac{e_{mix}}{D_{con} \rho_l \nu_l{}^2} \\
& e_{mix} = \tau_{mix} P_{a,STR} \Rightarrow \left[a_1 Re_{STR}{}^{b_1} \left(\frac{D_{con}{}^2}{\nu_l} \right) \right] \left[a_2 Re_{STR}{}^{b_2} \left(\left(n d_m \right)^3 d_m{}^2 \rho_l \right) \right] \qquad (22) \\
& \Rightarrow \left\{ \left(\frac{D_{con}{}^2}{\nu_l} \right) \left(\left(n d_m \right)^3 d_m{}^2 \rho_l \right) \left(\frac{\nu_l^2}{\nu_l^2} \right) \left(\frac{d_m}{d_m} \right) \right\} a_3 Re_{STR}{}^{b_3} \qquad \text{b} \\
& \Rightarrow e_{mix} = a_3 Re_{STR}{}^{3+b_3} \left\{ \frac{D_{con}{}^2 \rho_l \nu_l{}^2}{d_m} \right\} \\
& e^*_{mix} = a_3 Re_{STR}{}^{3+b_3} C^{b_3} = \frac{e_{mix}}{\frac{D_{con}{}^2 \rho_l \nu_l{}^2}{d_m}}
\end{aligned}
$$

3. Dissolution solid body in two reactor types

3.1. Literature survey

Many processes in chemical and related industries are carried out in heterogeneous solid–liquid systems. One of the most commonly used processes is the dissolution of a solid body in a liquid. The dissolution process of a solid body in a liquid can occur spontaneously or it can be intensified. One of the simplest methods of the mass transfer intensification is dissolution in mechanical mixers, i.e., apparatus with moving impellers [27,28]. Using the mechanical impeller should provide increase of the liquid turbulence, particularly at the boundary of the phases. The case of using mechanical mixers kinetic of the solid body dissolution depends on hydrodynamic conditions occurring inside the liquid volume, whereas hydrodynamics of the liquid depends on geometric configuration of the device. This is why the choice of the suitable impeller and mixing tank dimensions to the stirred medium, the type of the process, and the purpose of what we want to achieve are important issues. Except the result of research carried out for the well-known mechanical agitators, new constructional proposals of the mechanical mixers for performing solid dissolution process in a liquid can be found in the literature. This may have a positive effect on the mass transfer process, for example, using a reciprocating agitator [10,29–32]. Among other methods that are commonly used to intensify solid dissolution, a liquid pulsation [33], electrical discharges [34], other physical methods of the interaction [35], and dissolution on the solid or fluidized bed [36] can be found. In the case of dissolution process with chemical reaction an ultrasound can be used to the intensification [37–39]. In the last few years, a growth of interest in using of the magnetic fields in processes and unit operations in the scientific community was observed. Externally applied static magnetic field was used primarily to intensify the process of crystal growth [40,41] or during solidification

of metal alloys [42,43]. The rotating magnetic field can be successfully used in the crystallization process [44–47], fluidization [48,49], metallurgy [50,51], or even to increase the intensity of the dissolution process, as an alternative for mechanical mixing. This type of magnetic field induces azimuthal forces, which are time averaged. If the stirred liquid is magnetically susceptible, then azimuthal forces make a circumferential flow. Lines of the magnetic field rotate in a horizontal direction with rotation frequency of the field, ω_{RMF}. Moreover, the rotation frequency of the field is equal to frequency of an alternating current. An electric field, $\overline{E}$, is generated perpendicularly to the magnetic field, $\overline{B}$. The magnetic Lorentz forces, $\overline{F_n}$, which are perpendicular to the electrical field, act as driving forces for the rotating liquid. TRMF can be generated by a stator from three-phase asynchronous electric motor. This construction of the RMF generator was used in several studies [52,53]. When the stirred liquid is magnetically susceptible, then the RMF induces currents inside it. These currents interact with the field of the inductor. As a result, the electromagnetic forces inside the mixed liquor are generated. The pattern of the flow hydrodynamic induced by TRMF in the volume of the stirred liquid depends on the number of inductor pole pair, p_{TRMF}. RMF can be used to generate a specific flow in the cylindrical volume of the liquid. The liquid moves in a circumferential direction around the axis of the tank. This flow is directed the same as the direction of magnetic field rotations. Subsequently, the fluid velocity reaches the maximum value near to the tank wall, i.e., in the place characterized by the highest values of the magnetic induction. This movement may influence to the heat or mass transfer inside volume of the liquid. Analyzing the results that are available in the literature, it was found that research has not focused on a comparison between the mass transfer processes during the solid body dissolution realized in different systems: RMF mixers and stirred tank reactors. In this paper, experimental studies were conducted, and the effects of RMF and Rushton turbine on the solid body dissolution process in a liquid were compared.

3.2. Preparation of samples

As a solid body, the NaCl-cylindrical samples were used. To obtain suitable samples, i.e., samples that are dissolving in uniform manner, all of them were subjected to hardening process. First, raw rock salt cylinders were placed in a container filled up with a NaCl saturated solution. Second, after 24 h, the samples were pulled out and left dry. This process was repeated two times to obtain homogeneous and smooth surface of the cylindrical samples. A short thread stainless steel rod was glued to the top surface of the sample, which allows to mount it in a selected position in volume of the stirred liquid. Finally, the samples were securing at the bottom and top surface of the cylinder by applying a thin layer of glue on it. The prepared samples were used to perform the measurements.

Before the solubility measuring, the samples were hardened again in saturated salt solution during 60 s and then dried with paper. It was necessary because the dry samples may have to collect moisture from the stirred water, which could have a negative impact on the solubility process. Before each measurement the samples were weighed. Moreover, their height and diameter were measured. The diameter of the sample was measured at five different high levels located in equal increments and taken three times for different angular position of the sample. The location of the places where the diameter was measured is schematically shown in Figure 1.

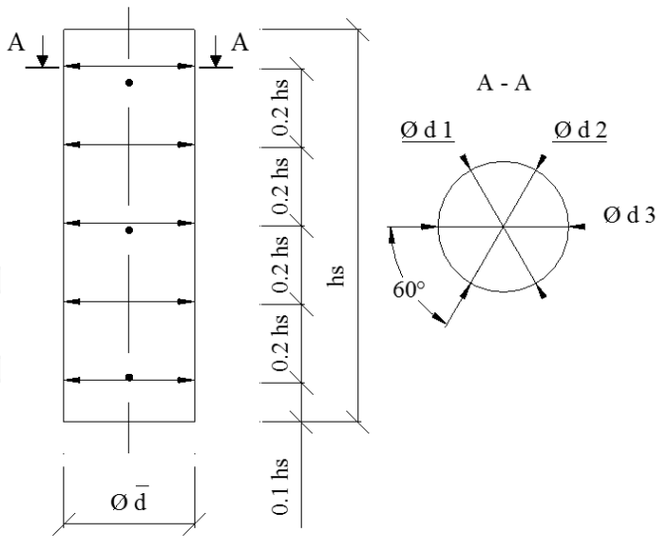

Figure 1. Location of the measurement levels on the solid sample.

Before the measurements in the magnetic stirrer were started, the magnetic field at a set point value of operating frequency of the stator was turned on. In the case of measurements for a mechanical mixer, first the impeller was set in motion on the requested rotation speed. Second, the conductivity measurement was switched. Then the sample was placed in a container filled up with tap water. In the case of a magnetic mixer, the sample was placed at the mid-height of electromagnetic laminations, where the most intensive magnetic field induction generated in a container takes place. Based on the literature data [54], it was found that it is also the place where the mass transfer process should proceed the fastest. The typical examples of the magnetic induction distribution in the form of the contours were presented in Figure 2.

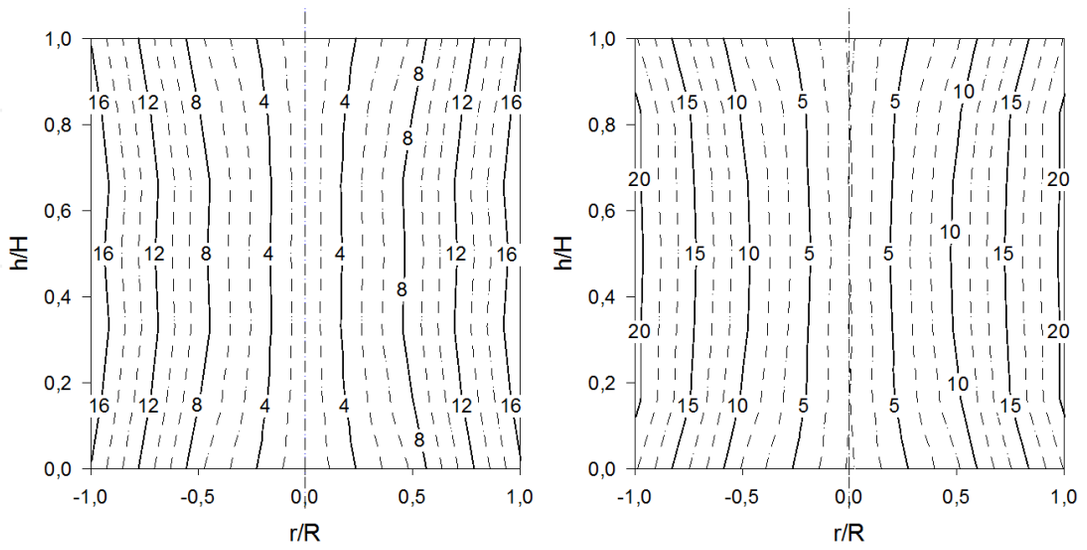

Figure 2. The typical example of the magnetic induction spatial distribution in the cross section of the RMF generator, f_{RMF} = 20 and 120 s^{-1}.

http://dx.doi.org/10.5772/61059

Every sample was dissolved once in short time equal to 5 s and then was pulled out of the system, dried by using the paper, measured, and weighed. For each sample, 13 replicates were performed. The number of repetition dissolution of the sample was chosen in a way to get appearance of the first pinholes. After the series of measurements, the data from multiparameter sensors were read. The water inside the container was replaced with a new one after every measurement series, keeping its temperature at constant level (T = 22–23°C).

3.3. Experimental setup

The first measurements of the NaCl-solid body dissolution were carried out in the RMF generator, which is shown in Figure 3. This experimental apparatus consists of a cylindrical glass container (2), a.c. transistorized inverter (3), and multifunctional computer meter (CX-701, Elmetron, Gliwice, Poland) (4). All of these elements are connected to the computer (5). The RMF generator was constructed of the stator, which was supplied from an electric motor with 50 Hz three-phase alternating current. The process parameters of the RMF generator were controlled using the special software. By controlling the inverter via a computer, it was possible to change the frequency of rotating magnetic field. In this case, the frequency was changed in the range of f = 2–120 s^{-1}. The glass container was placed inside of the RMF generator and filled up with the tap water to the volume equal to 16 dm^3. Conductivity was measured by means of the conductivity electrodes and the multifunction meters CX-701. Voltage signals were registered digitally every 0.1 s. The conductivity probe was positioned diagonally on the top and bottom of the glass container. The localization of the probes and the measurement points in the RMF generator are shown in Figure 4.

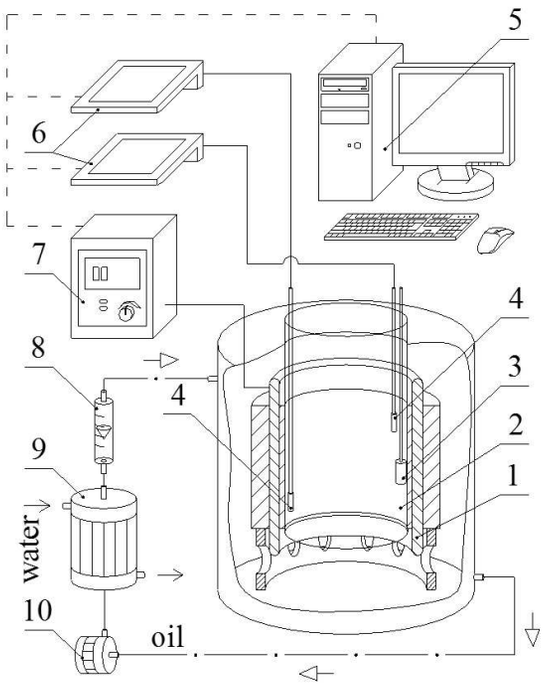

Figure 3. The sketch of the first experimental setup: 1—generator of rotating magnetic field, 2—glass container, 3—sample, 4—conductivity probes, 5—personal computer, 6—multifunctional computer meter, 7—a.c. transistorized inverter, 8—rotameter, 9—heat exchanger, 10—pump.

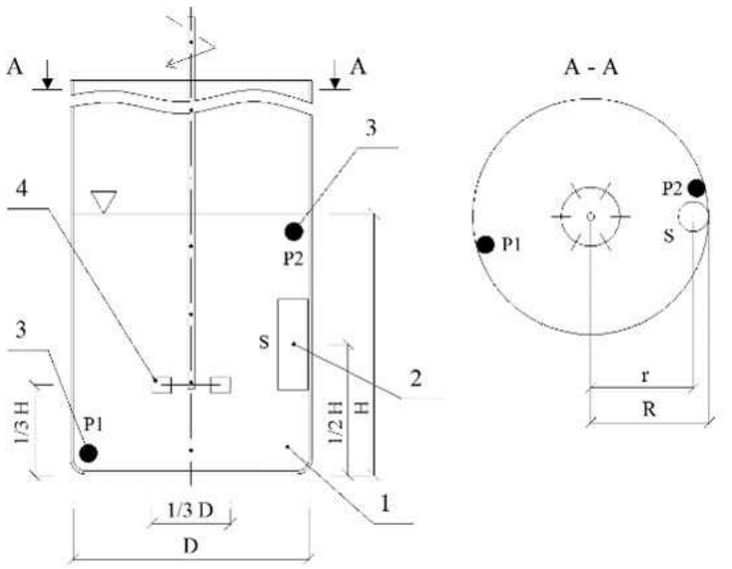

Figure 4. Localization of the probe and measurement points (where 1—glass container, 2—sample, 3—conductivity probes).

The second experimental apparatus are shown in Figure 5. It was the same glass vessel as in the first system; however, in this case, the mixing process was realized by using the mechanical high-speed impeller (Rushton disc turbine). The diameter of the agitator was equal to d_m = $0.33D_{con}$. The distance from the impeller center to the bottom of the vessel was $z = 0.33H$. The experiments were conducted at nine different values of impeller speed in the range of n = 0–3 s^{-1}. The measurement points correspond to those defined for the RMF generator (see Figure 4).

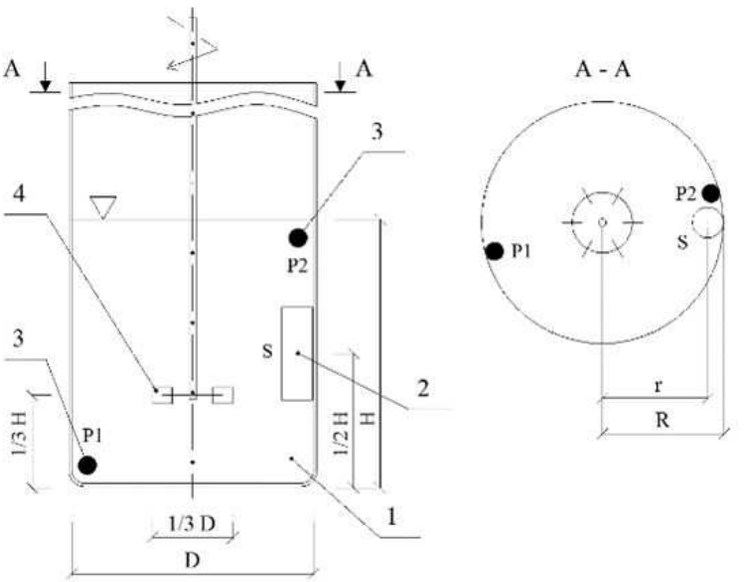

Figure 5. The sketches of the experimental setup with the mechanical mixer (where 1—glass container, 2—sample, 3—conductivity probes, 4—impeller).

http://dx.doi.org/10.5772/61059

3.4. Mixing time and power consumption measurements

The mixing time measurements for two systems were performed. The first mixer was under the action of the rotating magnetic field, and the second was equipped with the Rushton turbine mechanical impeller. The stirred vessel was filled up with a tap water (density 1000 kg m^{-3}, viscosity 1.002 mPa s, temperature 22–23°C). The geometric dimensions and process parameters for both systems are shown in Table 1.

Paramters	**Operating value**
Geometrical dimensions of mixer	
Vessel diameter, m	0.235
Agitator diameter, m	0.076
Time of dissolution, s	5
Height of liquid level in vessel, m	0.42
Operating conditions	
The frequency of rotation agitator, s^{-1}	0 – 3
Input power of agitator, W	0.002 - 26
Poles pair of generator RMF	2
The frequency of RMF, Hz	2 – 120
Input power of generator RMF, W	1 – 1050
Average diameter of sample, m	0.031
Average height of sample, m	0.074
Impulse temperature, °C	85
Electrical conductivity, $(\Omega m)^{-1}$	$2.5 \cdot 10^{-4}$

Table 1. The main geometrical dimensions of mixers and operation conditions

In this investigation, a thermal method was used to mixing time determination. First, a specific volume of the liquid with much higher temperature comparing to the mixed liquid was added to the system. As a tracer, a 0.3-dm^3 tap water with temperature equal to 85°C was used. Then changes of the liquid temperature were measured by using special experimental apparatus. It was an LM35 temperature sensor with measuring test card, which can process an analog signal in the form of the voltage to a digital signal. The voltage signal from the temperature probe was recorded at a frequency of 0.01 s. When the measurement was finished, a content of the glass container was poured out, and the vessel was filled up again with a new tap water characterized by the initial temperature. The mixing process was regarded as complete when the temperature fluctuations on one level were established. In this experiment, the end point was reached, when changes of the temperature at two measurement points were less than ±5% of the overall temperature increase. The mixing time, τ_{95}, was defined as the time after which

the temperature reaches a value equal to 95% of the final temperature of the liquid. It was assumed that this value of the mixing time will be achieved when the uniformity ratio of the temperature of the tracer, T_{tracer}, reaches a value equal to 0.05, according to the following equation:

$$T_{tracer} = \frac{T_\infty - T(\tau)}{T_\infty - T_0} \tag{23}$$

where T_0 is the initial temperature of the tracer, T_∞ is the final temperature of the stirred liquid, and $T(\tau)$ is the temperature at the measuring point at a time τ. The distribution of the temperature probes was analogous to the position of the conductivity probe in the mass transport process. Consequently, the point of the heat pulse dosing in the same place where the sample of the dissolved solid body was placed. Examples of the curves obtained from the mixing time measurements are shown in Figure 6.

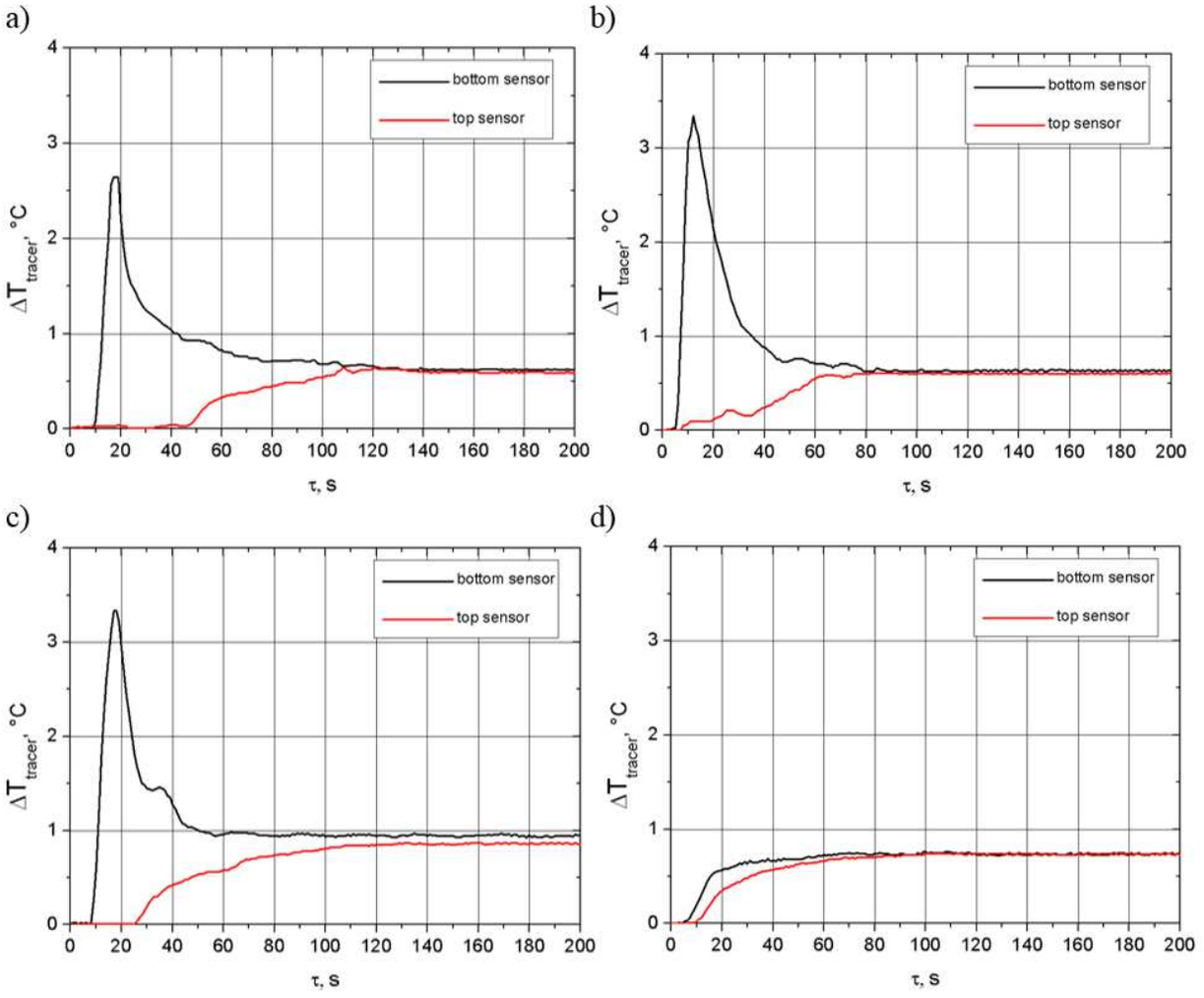

Figure 6. Typical example of temperature changes during mixing time investigations for (a) RMF $f = 20s^{-1}$, (b) $f = 120\ s^{-1}$, (c) mechanical agitator $n = 0.33\ s^{-1}$, and (d) mechanical agitator $n = 3\ s^{-1}$.

http://dx.doi.org/10.5772/61059

Additionally, measurements of the active power input to the test system with a mechanical stirrer and RMF were performed. In the case of the mechanical stirrer, it was possible to read power consumption directly from the digital display stirrer drive, whereas in the case of the system comprising an RMF generator, it has to be measured by using the electricity meter (type C-52 Pafal), located between the magnetic agitator and the a.c. transistorized inverter. The data that were collected were then graphically shown in Figure 7, in the form of the power change depending on an increasing rate of the rotational impeller speed. A similar relationship for the RMF is shown in Figure 8, except that in this case, the power depends on the frequency of magnetic field rotation change.

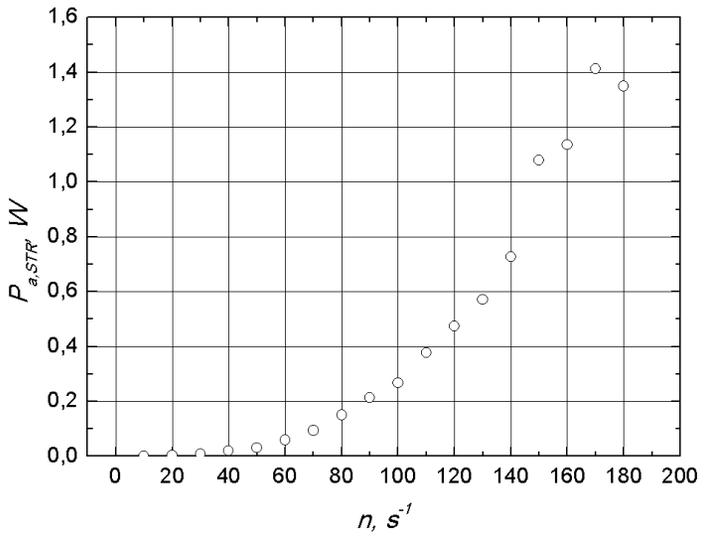

Figure 7. Power input measurements for mechanical mixer.

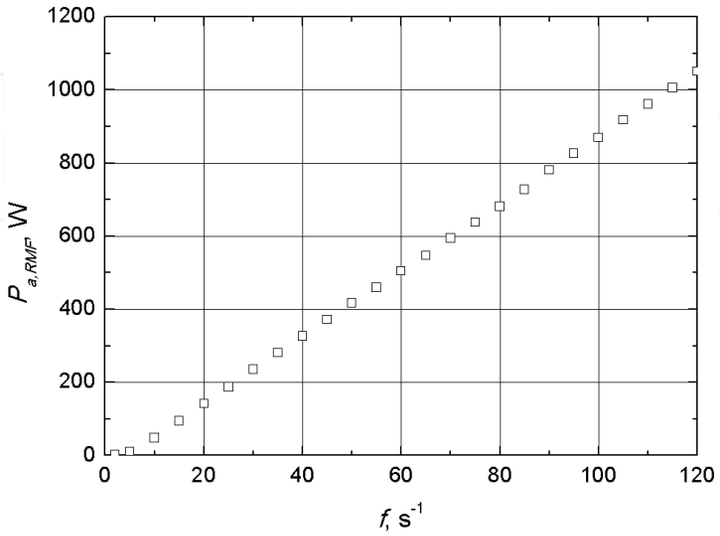

Figure 8. Power input measurements for the RMF generator.

4. Results and discussion

4.1. Influence of the Rushton turbine and the RMF on the mass transfer

The experimental results of the solid body dissolution are graphically shown in Figures 9 and 10. In Figure 9, results of the measurements for the mixing tank equipped with Rushton turbine impeller were presented. Furthermore, in the picture, an approximation of the experimental results and the proposed relationship were also presented. Analogous graph was prepared for the magnetic mixer and shown in Figure 10. Analyzing the plots, it was found that values of the mass transfer coefficients in the tested systems are depended on the Reynolds number. Additionally, a significant effect of the mixing method on the mass transfer process was observed. The higher impact of the Reynolds number value on the mass transfer coefficients in the STR was observed. In both systems, the mass transfer rate increased with increasing value of Reynolds number. However, the slope of the approximation curve was bigger in the case of the mechanical mixer than that in the case of the magnetic mixer. The proposed relationships were $Sh_{STR}\ Re_{STR}^{0.53}$ and $Sh_{RMF}\ Re_{RMF}^{0.26}$ for the STR and RMF generator, respectively.

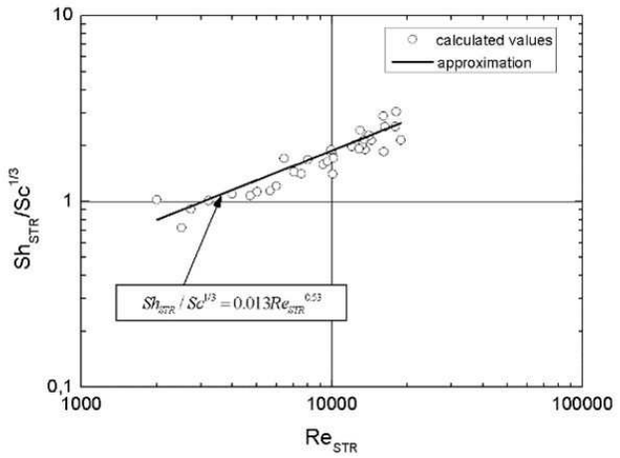

Figure 9. Mass transfer characteristics for Rushton turbine.

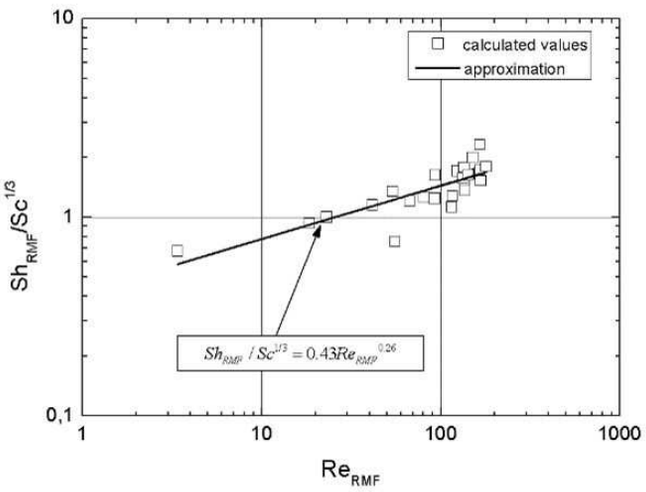

Figure 10. Mass transfer characteristics for the RMF generator.

http://dx.doi.org/10.5772/61059

4.2. Power characteristics for the Rushton turbine and the RMF

Power characteristics for both systems in Figures 11 and 12 were presented. As it could be seen, values of the power number for the STR system were much lower than those in the magnetic mixer. It is caused by the fact that in the case of the RMF generator, the power consumption was significantly higher, which consequently affects the calculated values of the Ne number. Based on the slope of the proposed approximation curve, in the case of mechanical mixer with increase value of the rotational impeller speed, the value of the Ne number was slightly decreasing. In the tested range, the proportionality $Ne_{STR}\ Re_{STR}^{-0.16}$ was found. A similar situation is in the case when the mixing process is carried out using the RMF generator. In that system, a slope of the approximation curve is also negative; however, the change in RMF frequency has a significant impact on the value of the Ne number. In the tested range, the proportionality $Ne_{RMF}\ Re_{RMF}^{-1.3}$ was found.

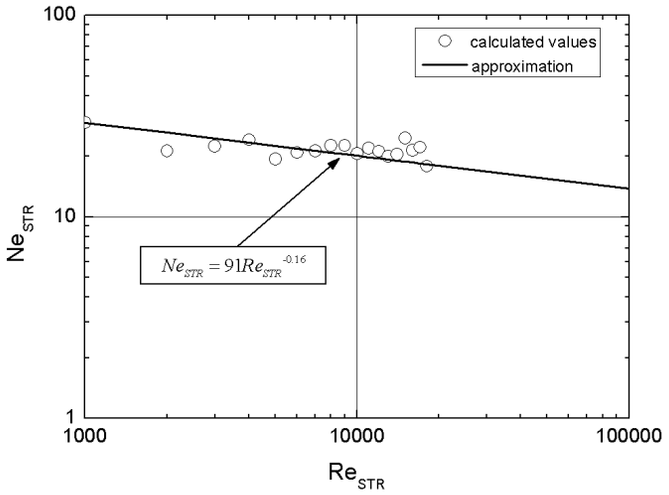

Figure 11. Power characteristic for Rushton turbine.

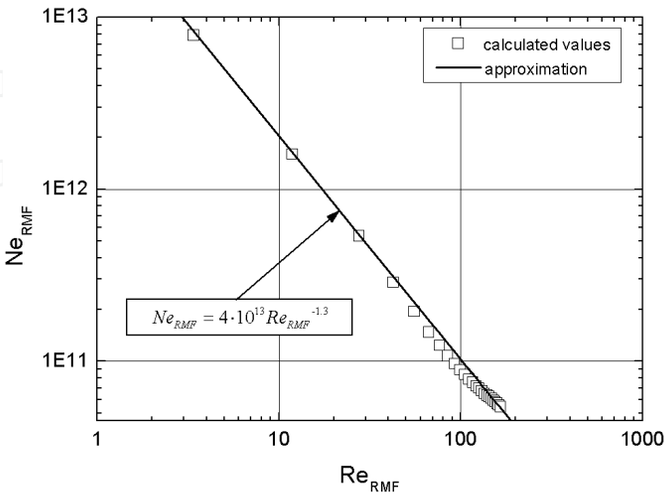

Figure 12. Power characteristic for the RMF generator.

4.3. Mixing time characteristics for the Rushton turbine and the RMF

In present consideration, the dimensionless mixing time was defined as

$$\Theta = \frac{\tau_0 \nu_0}{l_0^{\,2}} \Rightarrow \Theta = \frac{\tau_{mix} \nu_l}{D^2} \tag{24}$$

The mixing time may be analytically described using the relationship between the dimensionless mixing time and the Reynolds number. The experimental data obtained for the systems with the RMF generator or Rushton turbine in log–log graphs were presented (Figures 13 and 14). Analyzing the results shown in the graphs, it was found that values of the dimensionless mixing time decreased with increasing Reynolds number in both systems. Comparing results for both systems, it was found that smaller values of the dimensionless mixing time in the mixing process realized with using a Rushton turbine were obtained. Based on the curve slope, it can be assumed that the process using a mechanical impeller proceeds more intensively than that under the action of RMF. It should be noted that in the magnetic mixer, the process proceeds as a laminar, while the mechanical impeller induces a turbulent regime of the flow. According to that, using of an RMF mixer can be useful in a mixing process, when a turbulent flow of the fluid cannot be achieved, even if it will cause an increasing mixing time. An example can be here a bioprocess, where high shear forces connected with a turbulent flow can have a destructive impact on the microorganisms.

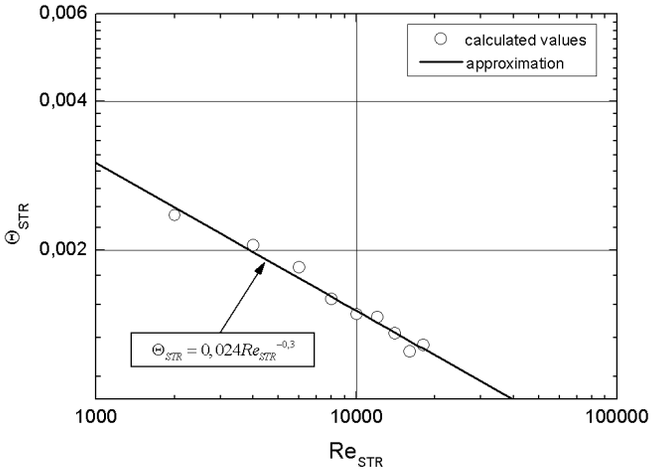

Figure 13. Dimensionless mixing time characteristic for Rushton turbine.

Additionally, values of the power number obtained from the experimental measurements and calculated on the basis of an approximating equation for the process under the action of the RMF are presented in the Figure 15 and compared.

http://dx.doi.org/10.5772/61059

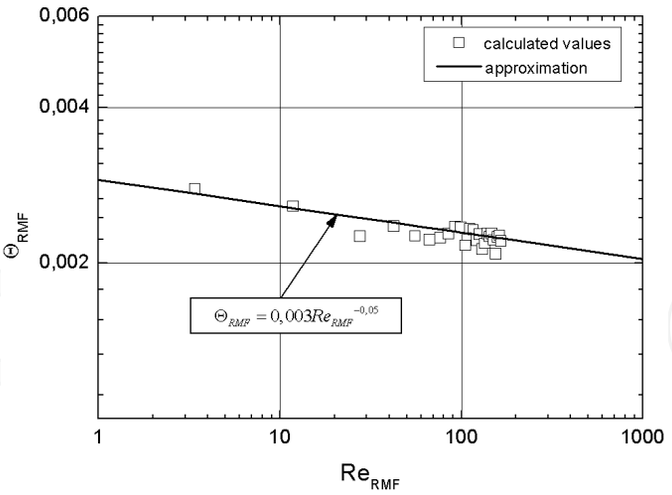

Figure 14. Dimensionless mixing time characteristic for the RMF generator.

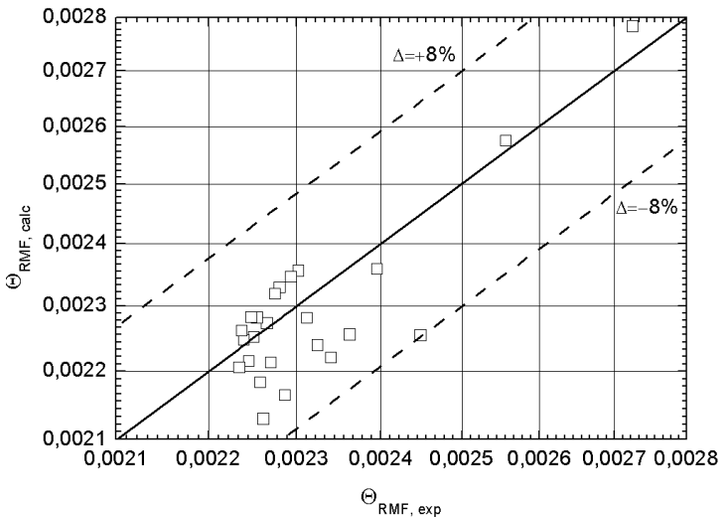

Figure 15. Comparison of the experimental and calculated values of the dimensionless mixing time for process under action of RMF.

5. Mixing energy

As mentioned before, an evaluation of the mixing process realized in different geometrical systems with a mixing energy parameter can be performed. Characteristics of the dimensionless mixing energy for both systems were graphically presented in Figures 16 and 17. As follows from the graphical analysis, lower values of the dimensionless mixing energy in the case of RT using were noted. The conclusion is that the rotational movements of mechanical impeller are more effective for the liquid mixing than the magnetic mixer in the whole tested range of the rotational impeller speed and RMF frequency. Nevertheless, the mixing process under the action of RMF is nonintrusive, which pose a huge advantage this type of mixer.

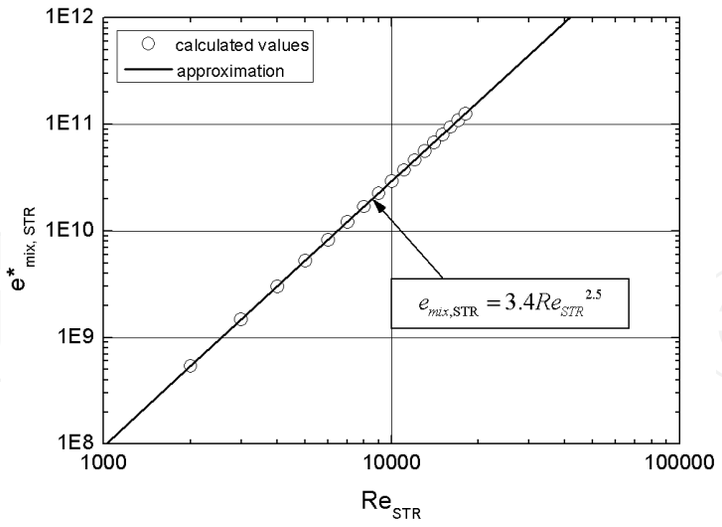

Figure 16. Dimensionless mixing energy characteristics for Rushton turbine.

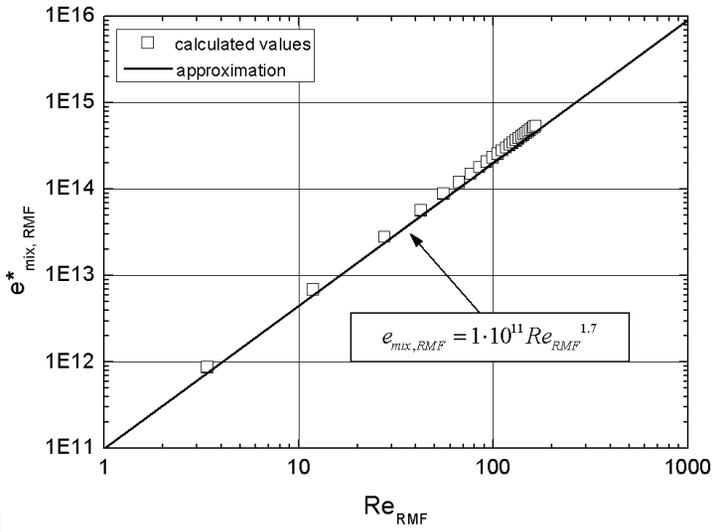

Figure 17. Dimensionless mixing energy characteristics for the RMF generator.

6. Conclusion

Obtained in this consideration, experimental and calculated results present an interesting effect of the rotating magnetic field and stirred tank reactor applications in the mass transfer process. Analyzing the obtained results reveals the following conclusions:

Values of the mass transfer coefficients increases with an increasing value of the rotational agitator speed and the magnetic field intensity. In the laminar regime of the flow, a stronger impact on the solid body dissolution in the case of magnetic mixer was observed, while in the

http://dx.doi.org/10.5772/61059

turbulent regime of the flow, better results in the stirred tank with mechanical RT impeller were obtained.

In the STR system, values of the power number were much lower than those in the magnetic mixer. Based on the proposed approximation curves slope, with the increasing value of the rotational impeller speed or RMF frequency, the value of the *Ne* number decreases.

In both systems, the dimensionless mixing time decreased with increasing value of the Reynolds number. However, smaller values of the dimensionless mixing time in the mixing process realized with using a Rushton turbine were obtained. It must therefore be concluded that the process carried out with using a mechanical impeller proceeds more intensively than that under the action of RMF.

On the basis of the dimensionless mixing energy comparison for both systems, it was found from the economical point of view that using of the rotating magnetic field is less profitable due to high power consumption. In the future, additional experimental measurements should be carried out for the system with the RMF generator in order to find a way to reduce the calculated values of dimensionless mixing energy. One of the possibilities is using of the magnetic particles, which can be added to the mixed liquid.

In order to better understand the mechanism of the mass transfer process under the action of the rotating magnetic field further studies, both theoretical and experimental should be carried out.

Nomenclature

B; magnetic induction; kg A^{-1} s^{-2}

D; diffusion coefficient; m^2 s^{-1}

D_{con}; diameter of glass container; m

d_m; diameter of Rushton turbine; m

d_s; diameter of sample; m

e_{mix}; mixing energy; J

f; frequency of RMF; s^{-1}

h; height of sample; m

H; liquid level in glass container;m

l; characteristic dimension; m

m; mass; kg

n; rotational speed of agitator; s^{-1}

Pa; active power; W

r,R; radius; m

T; temperature; °C

V; volume; m^3

Greek letters

$(\beta)_V$; volumetric mass transfer coefficient; kg m^{-3} s^{-1}

w; liquid velocity; m s^{-1}

w_{RMF}; liquid velocity under the action of RMF; m s^{-1}

η; dynamic viscosity ; kg m^{-1} s^{-1}

ν; kinematic viscosity; m^2 s^{-1}

ρ; density; kg m^{-3}

σ_e; electrical conductivity; A s^3 kg^{-1} m^{-3}

τ; time; s

ω_{RMF}; angular velocity of rotating magnetic field; rad s^{-1}

Ω; angular velocity of liquid in container; rad s^{-1}

Dimensionless number

e_{mix}*; dimensionless mixing energy

Ne; Newton number

Re; Reynolds number

Sc; Schmidt number

Sh; Sherwood number

Θ; mixing time number

Subscripts

0; reference value

L; liquid

P; conductivity probe

S; sample

Abbreviations

mix; Mixing

RMF; rotating magnetic field

STR; Rushton turbine

Author details

Grzegorz Story, Marian Kordas and Rafał Rakoczy*

*Address all correspondence to: rrakoczy@zut.edu.pl

Faculty of Chemical Engineering, Institute of Chemical Engineering and Environmental Protection Processes, West Pomeranian University of Technology, Szczecin, Szczecin, Poland

References

[1] Incropera, F.P., DeWitt, D.P. Fundamentals of Heat and Mass Transfer. USA: John Wiley & Sons Inc.; 2011. ISBN: 978-0470-50197-9

[2] Basmadjian, D. Mass Transfer. Principles and Applications.USA: CRC Press LLC; 2004. ISBN 9780203503140

[3] Bird, R.B.; Stewart, W.E., Lightfoot, E.N. Transport Phenomena.USA: Wiley; 1966. ISBN: 978-0471073925

[4] Kays, W.M., Crawford, M.E. Convective Heat and Mass Transfer. USA: McGraw-Hill; 1980. ISBN 9780070334571

[5] Garner, F.H., Suckling, R.D. Mass transfer form a soluble solid sphere. American Institute of Chemical Engineers Journal. 1958;4(1):114–124. DOI: 10.1002/aic.690040120

[6] Condoret, J.S.; Riba, J.P., Angelino, H. Mass transfer in a particle bed with oscillating flow. Chemical Engineering Science. 1989;44(10):2107–2111. DOI: 10.1016/0009-2509(89)85145-0

[7] Jameson, G.J.Mass (or heat) transfer form an oscillating cylinder. Chemical Engineering Science. 1964;19:793–800. DOI: 10.1016/0009-2509(64)85090-9

[8] Lemcoff, N.O., Jameson, G.J. Solid–liquid mass transfer in a resonant bubble contractor. Chemical Engineering Science. 1975;30:363–367. DOI: 10.1016/0009-2509(75)85001-9.3

[9] Noordsij, P., Rotte, J.W. Mass transfer coefficients to a rotating and to a vibrating sphere. Chemical Engineering Science. 1967;22:1475–1481. DOI: 10.1016/0009-2509(67)80073-33

[10] Tojo K., Miyanami K., Minami I. Vibratory agitation in solid–liquid mixing. Chemical Engineering Science. 1981;36:279–284. DOI: 10.1016/0009-2509(81)85006-3

[11] Sugano, Y., Rutkowsky, D.A. Effect of transverse vibration upon the rate of mass transfer for horizontal cylinder. Chemical Engineering Science. 1968;23:707–716. DOI: 10.1016/0009-2509(68)85005-5

[12] Wong, P.F.Y., Ko, N.W.M., Yip, P.C. Mass transfer from large diameter vibrating cylinder. Transactions of the Institution of Chemical Engineers. 1978;56(3):214–216. ISSN: 0371-7496

[13] Lemlich, R., Levy, M.R. The effect of vibration on natural convective mass transfer. American Institute of Chemical Engineers Journal. 1961;7:240–241. DOI: 10.1002/aic.690070214

[14] Woziwodzki Sz., Broniarz-Press L., Ochowiak M. Effect of eccentricity on transitional mixing in vessel equipped with turbine impellers. Chemical Engineering Research and Design. 2010;88(12):1607–1614.DOI:10.1016/j.cherd.2010.04.007

[15] Kuzmanić N., Ljubičić B. Suspension of floating solids with up-pumping pitched blade impellers; mixing time and power characteristics. Chemical Engineering Journal. 2001;84(3):325–333.DOI: 10.1016/S1385–8947(00)00382-X

[16] Kuzmanić N., Žanetić R., Akrap M. Impact of floating suspended solids on the homogenisation of the liquid phase in dual-impeller agitated vessel. Chemical Engineering Process. 2008;47(4):663–669. DOI: 10.1016/j.cep.2006.12.010

[17] Delaplace G., Leuliet J.C., Relandeau V. Circulation and mixing times for helical ribbon impellers. Review and experiments. Experiments in Fluids. 2000;28:170–182. DOI: 10.1007/s003480050022

[18] Karcz J., Cudak M., Szoplik J. Stirring of a liquid in a stirred tank with an eccentrically located impeller. Chemical Engineering Science 2005;60(8–9):2369–2380. DOI: 10.1016/j.ces.2004.11.018

[19] Masiuk S. Mixing time for a reciprocating plate agitator with flapping blades. Chemical Engineering Journal 2000;79(1):23–30. DOI: 10.1016/S1385-8947(00)00141-8

[20] Zlokarnik M. Stirring—Theory and Practice. Weinheim: Wiley-VCH Verlag; 2001. ISBN 978-3-527-29996-3

[21] Harnby N., Edwards M.F., Nienow A.W. Mixing in the Process Industries. 2nd ed.UK: Butterworth-Heinemann, 2000.

[22] Rakoczy R. Mixing energy investigations in a liquid vessel that is mixed by using a rotating magnetic field. Chemical Engineering and Processing. 2013;66:1–11. DOI: 10.1016/j.cep.2013.01.012

[23] Masiuk, S., Kawecka-Typek, J. Mixing energy measurements in liquid vessel with pendulum agitators. Chemical Engineering and Processing. 2004;43(2):91–99. DOI: 10.1016/S0255-2701(03)00072-2

[24] Masiuk, S., Rakoczy, R., Kordas, M. Comparison density of maximal energy for mixing process using the same agitator in rotational and reciprocating movements. Chemical Engineering and Processing. 2008;47(8):1252–1260. DOI: 10.1016/j.cep.2007.04.004

[25] Nienow, A.W. On impeller circulation and mixing effectiveness in the turbulent flow regime. Chemical Engineering Science. 1997;52(15):2557–2565. DOI: 10.1016/S0009-2509(97)00072-9

[26] Bouaifi M., Roustan M. Power consumption, mixing time and homogenisation energy in dual-impeller agitated gas–liquid reactors. Chemical Engineering and Processing. 2001;40(2):87–95, DOI: 10.1016/S0255-2701(00)00128-8

[27] Hörmann T., SuzziD., Khinast J.G. Mixing and dissolution processes of pharmaceutical bulk materials in stirred tanks: experimental and numerical investigations. Industrial and Engineering Chemistry Research. 2011;50(21):12011–12025. DOI: 10.1021/ie2002523

[28] Hartmann H., Derksen J.J., van den Akker H.E.A. Numerical simulation of a dissolution process in a stirred tank reactor. Chemical Engineering Science. 2006;61:3025–3032. DOI: 10.1016/j.ces.2005.10.058

[29] Baird M.H.I., Rama Rao N.V., Vijayan S. Axial mixing and mass transfer in a vibrating perforated plate extraction column. Canadian Journal of Chemical Engineering. 1992;70:69–76. DOI: 10.1002/cjce.5450700111

[30] Kordas M., Rakoczy R., Grądzik P., Story G. Rozpuszczanie ciała stałego w mieszalniku z mieszadłem wykonującym ruch obrotowy i posuwisto-zwrotny. Inżynieria i Aparatura Chemiczna. 2012;51(6):346–347. (In Polish).

[31] Masiuk S. Dissolution of solid body in a tubular reactor with reciprocating plate agitator. Chemical Engineering Journal. 2001;83:139–144. DOI: 10.1016/S1385-8947(00)00268-0.

[32] Masiuk S., Rakoczy R. Power consumption, mixing time, heat and mass transfer measurements for liquid vessels that are mixed using reciprocating multiplates agitators. Chemical Engineering and Processing. 2007;46:89–98. DOI:10.1016/j.cep.2006.05.002

[33] NiX., GaoS. Scale-up correlation for mass transfer coefficients in pulsed baffled reactors. Chemical Engineering Journal and the Biochemical Engineering Journal. 1996;63(3):157–166. DOI:10.1016/S0923-0467(96)03120-X

[34] Coteaţă M., Schulze H.P., Slătineanu L. Drilling of difficult-to-cut steel by electrochemical discharge machining. Materials and Manufacturing Processes. 2011;26(12):1466–1472. DOI: 10.1080/10426914.2011.557286

[35] Tai C.Y., Chi-Kao W., Chang M.C. Effects of magnetic field on the crystallization of $CaCO_3$ using permanent magnets. Chemical Engineering Science. 2008;63:5606–5612. DOI: 10.1016/j.ces.2008.08.004

[36] Kalaga D.V., Dhar A., Dalvi S.V., Joshi J.B. Particle–liquid mass transfer in solid–liquid fluidized beds. Chemical Engineering Journal. 2014;245:323–341. DOI:10.1016/j.cej.2014.02.038

[37] Grénman H., Murzina E., Rönnholm M., Eränen K., Mikkola J., Lahtinen M., et al. Enhancement of solid dissolution by ultrasound. Chemical Engineering and Processing. 2007;46:862–869. DOI:10.1016/j.cep.2007.05.013

[38] Kannan A., Pathan S.K. Enhancement of solid dissolution process. Chemical Engineering Journal. 2004;102:45–49. DOI: 10.1016/j.cep.2009.11.004

[39] Sandilya K.D., Kannan A. Effect of ultrasound on the solubility limit of a sparingly soluble solid. Ultrasonics Sonochemistry. 2010;17:427–434. DOI:10.1016/j.ultsonch. 2009.10.005

[40] Dold P., Szofran F.R., Benz K.W. Thermoelectromagnetic convection in vertical Bridgman grown germanium–silicon. Journal of Crystal Growth. 2006;291:1–7. DOI: 10.1016/j.jcrysgro.2006.02.055

[41] Kao, A., Djambazov, G., Pericleous, K. and Voller, V. Effects of magnetic fields on crystal growth. Proceedings in Applied Mathematics and Mechanics. 2007;7:4140015–4140016. DOI: 10.1002/pamm.200700922

[42] Du D., Hou L., Gagnoud A., Ren Z., Fautrelle Y. Cao G., Li X. Effect of an axial high magnetic field on Sn dendrite morphology of Pb–Sn alloys during directional solidification. Journal of Alloys and Compounds. 2014;588:190–198. DOI:10.1016/j.jallcom. 2013.11.011

[43] Bouabdallah S., Bessaïh R. Effect of magnetic field on 3D flow and heat transfer during solidification from a melt. International Journal of Heat and Fluid Flow. 2012;37:154–166. DOI: 10.1016/j.ijheatfluidflow.2012.07.002

[44] Spitzer K.H. Application of rotating magnetic field in Czochralski crystal growth. Progress in Crystal Growth Characterization. 1999;38(1–4):59–71. DOI: 10.1016/S0960-8974(99)00008-X

[45] Dold P., Benz K.W. Rotating magnetic field: fluid flow and crystal growth applications. Progress in Crystal Growth Characterization of Materials. 1999;38:7–38, DOI 10.1016/S0960-8974(99)00007-8

[46] Walker J.S. Bridgman crystal growth with a strong, low-frequency, rotating magnetic field. Journal of Crystal Growth. 1998;192(1–2):318–327. DOI:10.1016/S0022-0248(98)00438-2

[47] Yang, M., Ma, N., Bliss, D.F., Bryant G.G. Melt motion during liquid-encapsulated Czochralski crystal growth in steady and rotating magnetic field. International Journal of Heat and Mass Transfer. 2007;28:768–776. DOI: 10.1016/j.ijheatfluidflow. 2006.08.001

[48] Lu, X.S., Li, H. Fluidization of $CaCO_3$ and Fe_2O_3 particle mixtures in a transverse rotating magnetic field. Powder Technology. 2000;107:66–78. DOI: 10.1016/S0032-5910(99)00092-3

[49] Hristov J. Magnetic field assisted fluidization—dimensional analysis addressing the physical basis. China Particuology. 2007;5(1–2):103–110. DOI:10.1016/j.cpart.2007.03.002

[50] Nikrityuk, P.A., Eckert, K., Grundmann, R. A numerical study of unidirectional solidification of a binary metal alloy under influence of a rotating magnetic field. International Journal of Heat and Mass Transfer. 2006;49:1501–1515. DOI: 10.1016/j.ijheatmasstransfer.2005.08.035

[51] Willers, B., Eckert, S., Michel, U., Haase, I., Zouhar, G. The columnar-to-equiaxed transition in Pb–Sn alloys affected by electromagnetically driven convection. Materials Science and Engineering A. 2005;402(1–2):55–65, DOI: 10.1016/j.msea.2005.03.108

[52] Lu, X.S., Li, H. Fluidization of $CaCO_3$ and Fe_2O_3 particle mixtures in a transverse rotating magnetic field. Powder Technology. 2000;107:66–78. DOI: 10.1016/S0032-5910(99)00092-3

[53] Rakoczy, R., Masiuk, S. Influence of transverse rotating magnetic field on enhancement of solid dissolution process. American Institute of Chemical Engineers Journal. 2010;56:1416–1433. DOI: 10.1002/aic.12097

[54] Rakoczy R. Enhancement of solid dissolution process under the influence of rotating magnetic field. Chemical Engineering and Processing: Process Intensification. 2010:49(1):42–50. DOI: 10.1016/j.cep.2009.11.004

IntechOpen

IntechOpen

IntechOpen